Controllable current oscillation and pore morphology evolution in the anodic growth of TiO_2 nanotubes

2011 Nanotechnology 22 155603

(http://iopscience.iop.org/0957-4484/22/15/155603)

Nanotechnology **22** (2011) 155603 (12pp) doi:10.1088/0957-4484/22/15/155603

Controllable current oscillation and pore morphology evolution in the anodic growth of TiO_2 nanotubes

Hong Liu, Liang Tao and Wenzhong Shen[1]

Laboratory of Condensed Matter Spectroscopy and Opto-Electronic Physics and Key Laboratory of Artificial Structures and Quantum Control (Ministry of Education), Department of Physics, and Institute of Solar Energy, Shanghai Jiao Tong University, 800 Dong Chuan Road, Shanghai 200240, People's Republic of China
and
Institute of Solar Energy, Shanghai Jiao Tong University, 800 Dong Chuan Road, Shanghai 200240, People's Republic of China

E-mail: wzshen@sjtu.edu.cn

Received 4 November 2010, in final form 10 February 2011
Published 10 March 2011
Online at stacks.iop.org/Nano/22/155603

Abstract

The spatial heterogeneities and temporal instabilities in the anodic growth of TiO_2 tubes are very important for nanostructure fabrication, but few ordered cases have been reported. In this work, we represent a new current oscillation with pore morphology evolution in the formation of anodic TiO_2 tubes. Small (less than 8.0% of the minimum value) and fast (period $\sim 10^0$ s) current oscillation was formed under static conditions in a wide range, while significant morphological change such as periodical narrowing, abruption and small pits appeared in the pore with characteristic length scale of 10^1–10^2 nm. Surprisingly, the roughness in the pore would be totally eliminated instead of being enhanced by high speed stirring or periodically modulated voltage with the current oscillation still being enhanced, which indicates an important involvement of the ion transport process. It has also been found that the growth rate could be significantly accelerated by tuning the stirring rate or the periodical modulation of the voltage. The mechanism has been described with consideration of the local reactions and the ion transport with a key involvement of the convection process, which can be strongly influenced by the mechanical stirring and the modulated voltage.

(Some figures in this article are in colour only in the electronic version)

1. Introduction

The nanostructures of metal oxides from valve metals (Al, Hf, Nb, Ta, Ti, W, Zr) have attracted tremendous attention over the past years due to their rich physical and chemical properties with widespread novel applications. Among them anodic TiO_2 tubes have received considerable interest since they were reported by Zwilling *et al* [1]. Due to their wide band semiconductivity with high aspect ratio and catalytic properties with a large efficient surface, the TiO_2 tubes have become very useful in water splitting [2], dye-sensitized solar cells (DSSCs) [3, 4], electrochromic display devices [5], photocatalysis [6] and some biomedical uses [7–9]. In recent years, electrochemical anodization under potentiostatic or galvanostatic conditions has been widely applied not only to the growth of long-range ordered TiO_2 nanotube arrays [10–14], but also to the nanostructure fabrication of other materials, for example porous anodic aluminum oxide [15–17].

Normally, two tasks are very important in the synthesis of the anodic nanostructures: (1) the controlled growth of tubes with high quality and growth rate; (2) the development of new functional structures. Many experiments have been carried out for the first issue and many valuable experimental results have been discovered. These results include the involvement

[1] Author to whom any correspondence should be addressed.

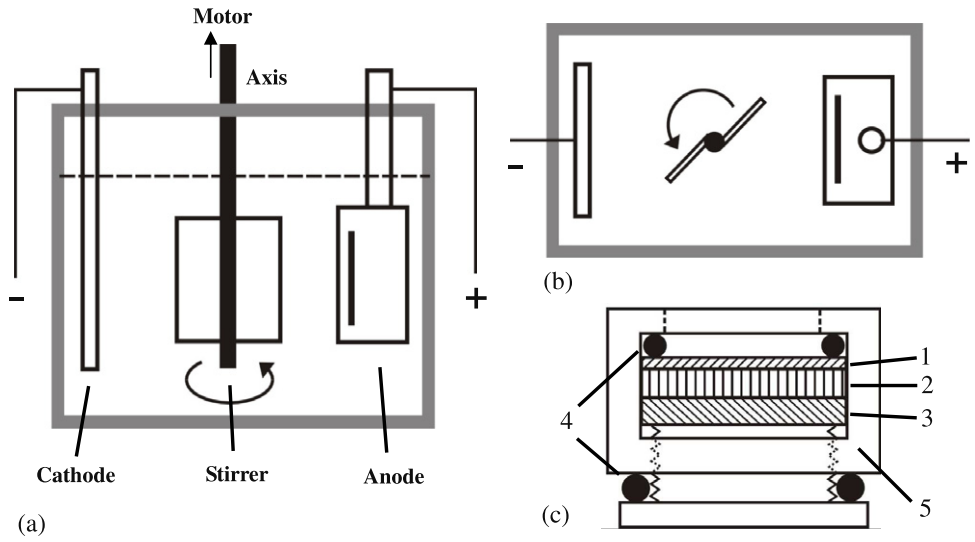

Figure 1. Schematic description of the experimental setup: (a) apparatus with stirring, cross-sectional view; (b) apparatus with the agitator, top view; (c) structure of the anode, cross-sectional view. (1) Ti plate, (2) copper electrode, (3) copper plate, (4) rubber O-ring, (5) outer shell.

of separated factors (anodic voltage, water content and pH value) [18–22], the application of organic electrolyte [23–26], quality improvement by a second anodization [27] and the gravity effect on tube growth [28]. For the second issue, some new structures have been created with several key factors being modified [29–31], such as nanolaces and 'bamboo-type' structures [32]. New applications of these structures have also been studied [33].

Based on those extensive results, deeper studies on more complicated behaviors under coaction of the key factors in a realistic reaction process have become possible in recent years. One of the most interesting phenomena is the spontaneous oscillation behavior in the electrolysis systems. For instance, slow (characteristic time $t_c \sim 10^0$ min) voltage oscillation was discovered in the galvanostatic anodic TiO_2 formation [34], which was claimed to be related to the detachment of the tube array from the substrate surface [34–36]. Another example is the faster ($t_c \sim 10^0$–10^1 s) current oscillation in the porous Al_2O_3 formation under potentiostatic conditions [37], which was claimed to be related to the oxidation process controlled by diffusion throughout the pore. Such phenomena have revealed remarkable characteristics of the anodization systems of Ti and other valve metals, which should be related to some more detailed processes. Consequently, processes such as the local reactions, diffusion and field-aided transport processes of the species (F^-, O^{2-}, TiO_2) are considerable for these systems which are far from equilibrium [30, 38, 39]. With comprehension of the mechanism, the whole process can be better controlled in some sense by tuning the key factors.

In this paper, we report a new kind of spatio-temporal oscillatory behavior in the TiO_2 anodic growth under potentiostatic conditions. It generally consists of small current oscillation in a short characteristic timescale ($t_c \sim 10^0$ s) with low magnitude ($<8.0\% j_{min}$) and the morphological change in the pore area with characteristic length scale of $\sim 10^1$–10^2 nm. This phenomenon can exist under a wide range of conditions, which can be an important factor that has influenced the quality of the fabricated tube arrays.

Moreover, the ordering and magnitude of the oscillation could be effectively influenced when tuning the macroscopic experimental conditions (the stirring rate and modulation of the voltage) in a certain way. One interesting phenomenon is that when enhancing these conditions, the spatial heterogeneity in the pore area of the tubes could be totally eliminated instead of being enhanced. Furthermore, the mechanical stirring and periodically modulated voltage can also significantly accelerate the tube growth. The mechanism during the whole process has been discussed with consideration of the reaction and diffusion processes of the reaction species [38, 39]. As a general result, an effective control of the tube formation can be realized by tuning the stirring rate and modulated voltage, which function as tunable ion pumps. Very ordered, smooth and straight TiO_2 tube arrays with quite thin wall thickness can be fabricated with a high growth rate, which can be useful in a broad range of applications. Additionally, TiO_2 tubes with a certain periodicity in the pore could also be synthesized by this controlling method, which might be applied as a functional material or a template for nanostructure synthesis.

2. Experimental section

The substrates are round Ti discs with diameter of 20 mm, which were originally cut from a Ti plate (thickness 0.25 mm, Sigma-Aldrich, 99.7%). These discs were chemically cleaned with an ultrasonic bath in methanol, acetone and isopropanol, followed by subsequent rinsing in de-ionized water and drying with air.

Electrochemical anodization was performed in a two-electrode configuration as shown in figures 1(a) and (b), using a direct current power supply (Agilent 5720) and a Keithley 2400 sourcemeter to measure the resulting current. The Ti discs were mounted in the anode chamber sealed by two O-rings, as shown in figure 1(c), with an area of about 1.767 cm^2 exposed to the

electrolyte. The stirring was driven by an external motor that rotates the electrolyte between the electrodes, with the stirring rate adjusted from 0 to 820 rpm by an electronic controller. The anodization was started with an initial voltage ramping and then kept at a certain constant voltage for 1 h.

In order to investigate the universality of the results, experiments were carried out at temperature between −5 and 15 °C. Experiments on the influence of the stirring rate and the voltage were mostly conducted at 5 °C. The applied electrolyte was ethylene glycol with 0.09 M NH_4F and different water concentrations (specified in different figures). After the anodization, the fabricated TiO_2 tube arrays were examined by the field emission scanning electron microscopes (FE-SEM, XL30FEG from Philips and SIRION200 from FEI) and the transmission electron microscope (TEM, JEM2100 from JEOL).

3. Results and discussion

3.1. The current oscillation and the pore morphological change in the formation of the anodic TiO_2 nanotubes

During the anodic growth of TiO_2 nanotubes under potentiostatic conditions in ethylene glycol, a new type of current oscillation was discovered. This oscillation had quite small amplitude (less than 8.0% minimum current density) and high frequency ($\sim 10^{-1}$ Hz), and appeared at both high and low anodization potentials. At high voltage, the oscillation period remained almost constant at about 5.0–6.0 s during the growth, as shown in figure 2(a). Its magnitude was about 0.9–1.1 mA cm^{-2}, which was 1.3–1.8% of the minimum current density. At low voltage, as shown in figure 2(b), the period of the oscillation changed from ∼9.0 s at the beginning to ∼7.0 s at the end. In the mean time, the magnitude of the oscillation was only 3.4×10^{-3}–6.8×10^{-3} mA cm^{-2}, which was about 0.17–0.25% of the minimum current density. Generally, the overall characteristic timescale of the current oscillation was 4.0–9.5 s, about two orders of magnitude smaller than the voltage oscillation in titanium anodization under galvanostatic conditions [36]. The period of the oscillation has only slightly changed during the long period of the anodization with quite small amplitude (less than 8.0% of the minimum current density), which is also significantly different from the current oscillation in the potentiostatic anodization of aluminum [38].

Although the amplitude of the current oscillation is small, significant pore morphological change can exist in the anodic TiO_2 nanotubes, as shown by the TEM images in figures 2(c)–(f). In the meantime, no significant spatial changes were observed in the copper cathode surface, therefore only the titanium substrate in the anode became the site of interest. Different structures could be formed in the pore of the TiO_2 tubes, such as the periodical narrowing (figure 2(c)), abruptions (figure 2(d)) and small pits on the inner surface (figure 2(e)), normally with a characteristic length scale of $\sim 10^1$–10^2 nm. These spatial changes in the pore are not significantly correlated to the 'bamboo-type' structure with certain periodicity outside the tubes in previous reports [32, 40], as shown with the pore images by TEM in figure 2(f). Apparently, some intrinsic relationship might exist between the current and morphological behaviors, as indicated in figure 2. However, no significant synchronization could be detected between the j–t curve and the pore morphology in most situations. Therefore, it is necessary to study the origin and properties of such phenomena in more detail.

Before more detailed investigation, it is important to choose the key controlling factors. The previous studies have shown that the tube growth could be significantly influenced by many factors such as the pH value, temperature, water content, anodic voltage and stirring conditions [18, 20–33, 37]. Among these factors, the mechanical stirring and the anodic voltage are the most controllable ones that can be easily modulated in a short timescale ($\sim 10^0$ s). On one hand, as an often applied method in electrochemical systems, stirring is helpful to study the possible origins of the current oscillation and the pore morphology change, for example the outer mechanical vibrations. On the other hand, the anodic voltage with modulations can also help to diagnose possible involvement of electrical factors, for example noise in the electronic instruments. Therefore, mechanical stirring and anodic voltage are quite suitable factors to investigate the oscillatory behavior in the TiO_2 anodic system.

3.2. The effect of mechanical stirring on the current oscillation and the pore morphology

Experiments on the influence of mechanical stirring have been generally carried out under high field conditions in order to obtain a high growth rate. Figures 3(a) and (b) have shown interesting results of the current oscillation and the pore morphological change with different stirring rates at a constant voltage. When the stirring rate Φ was zero, the current oscillation still existed but with a quite low amplitude ($\sim 0.1\% j_{\min}$). As the stirring rate was increased (for example, at $\Phi = 160$ rpm), the amplitude of the current oscillation rose up and its ordering became gradually better, as shown in figure 3(b). When $\Phi = 410$ rpm, the current oscillation became most ordered with higher amplitude ($\sim 2.9\% j_{\min}$). When the stirring rate reached 512 rpm, the current oscillation rapidly turned chaotic with further increased amplitude ($\sim 4.4\% j_{\min}$). With higher stirring rate (for example $\Phi = 820$ rpm), the current oscillation became more chaotic and its amplitude became even stronger. In the mean time, the average current density decreased with the increasing stirring rate. The overall characteristic timescale of these oscillations remained within the range of 4.0–9.5 s, almost two orders of magnitude higher than the period of stirring (∼0.1 s).

The morphological studies have shown quite sophisticated results, as demonstrated by the TEM images presented in figure 3(b). As the mechanical stirring was applied, the inner morphological change became less chaotic. When the stirring rate reached the medium value ($\Phi = 410$ rpm), some spatial periodicity appeared in the inner surface of the tubes together with ordered current oscillation, as also shown in the TEM images in figure 2. However, when the stirring rate was further increased ($\Phi = 512$ rpm), the roughness on the pore surface began to vanish drastically. Finally, the inner surface of the

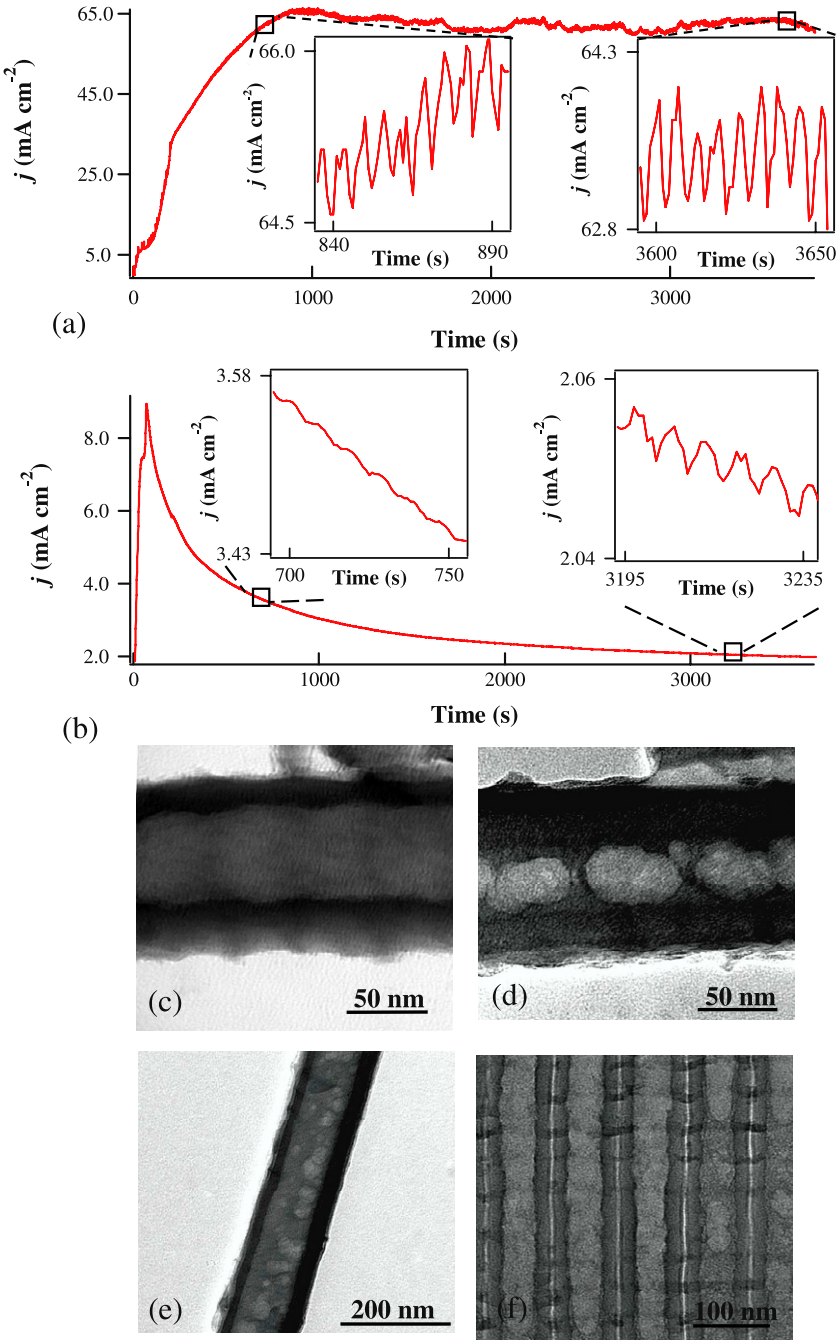

Figure 2. The current oscillation and pore morphological change in the potentiostatic anodization of TiO_2 tubes in ethylene glycol (0.09 M NH_4F) at 5 °C. (a), (b) *j*–*t* curve at 210.0 V and 70.0 V, respectively, stirring rate $\Phi = 410$ rpm. (c)–(e) TEM images showing the morphology in the pore area: (c) periodical narrowing (220.0 V, 1.0 vol% H_2O), $\Phi = 410$ rpm, with growth rate 9.0 nm s^{-1}; (d) periodical separating (180.0 V, 2.2 vol% H_2O), $\Phi = 410$ rpm, with growth rate 14.6 nm s^{-1}; (e) shallow pits on the inner surface (230.0 V, 2.2 vol% H_2O), $\Phi = 410$ rpm, with growth rate 3.0 nm s^{-1}. (f) TEM image, showing the inner and outer morphology (190 V, 1.0 vol% H_2O), $\Phi = 205$ rpm, with growth rate 6.0 nm s^{-1}.

TiO_2 tube wall became totally smoothed when the stirring rate became very high ($\Phi = 820$ rpm). Generally, the rough inner surface of the tubes still existed even with the weak current oscillation without stirring, whereas very smooth pore surface would exist with very strong current oscillation. This phenomenon has clearly indicated that there is no simple correlation between the total current oscillation and the pore morphology change of the TiO_2 tubes.

The above results have shown how the oscillatory behavior changed with constant stirring rates. A 'switching experiment' was then carried out to investigate the changes taking place in the oscillation (oscillation ordering, magnitude and average current density) with rapidly switched stirring conditions, as shown in figure 4. In the beginning, the anodization was started at a constant voltage without stirring. When the current was stable, the stirring was quickly switched on, and then kept at

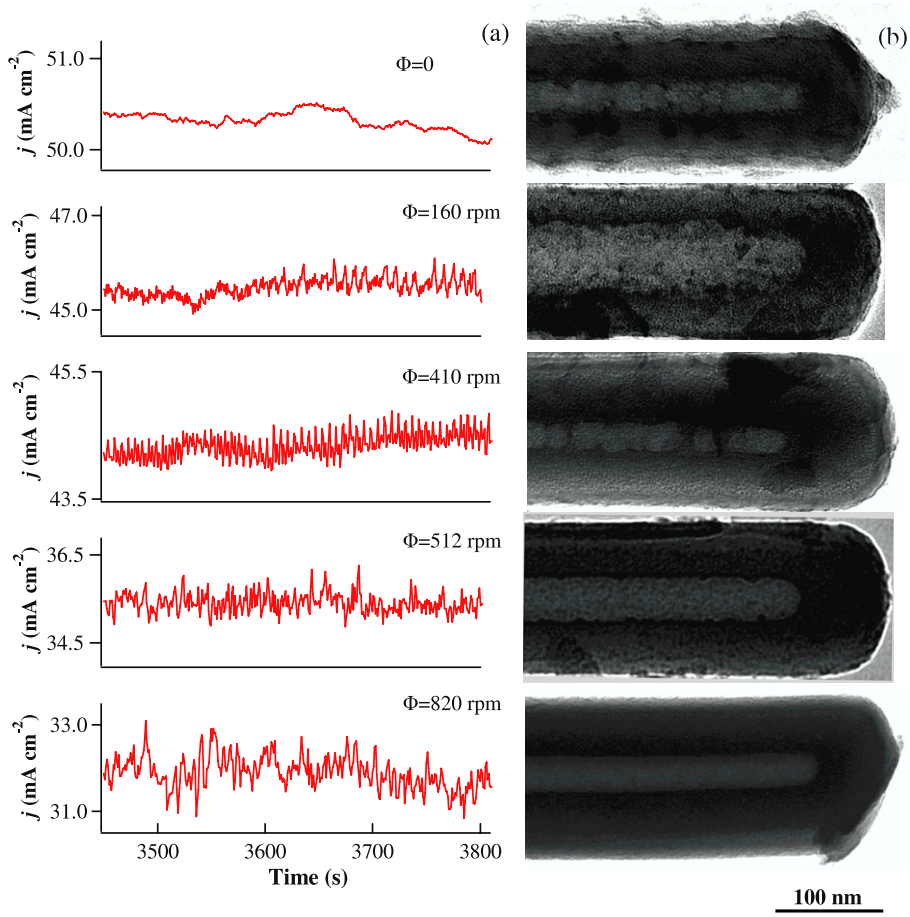

Figure 3. The current oscillation and corresponding inner morphology at different stirring rates, with the anodization time $t_a = 3600$ s, at 210.0 V, 5 °C. (a) The j–t curve in different stirring rates; (b) the TEM images of the bottom area of the TiO_2 tubes at different stirring rates, cross-sectional view.

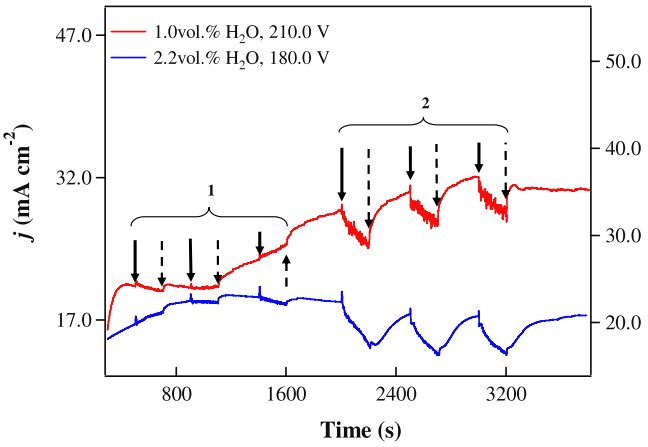

Figure 4. The j–t curves from the 'switching experiment', $T = 5$ °C. The solid and dashed arrows indicate the switching on and off of the stirring, respectively. The red and blue curves represent the results from experiments under different conditions (1.0 vol% H_2O at 210.0 V and 2.2 vol% H_2O at 180.0 V). (1) First procedure with $\Phi = 410$ rpm, (2) second procedure with $\Phi = 820$ rpm.

constant values for 3 min before being turned off. Such an operation was repeated three times in two procedures (marked by braces 1 and 2 in figure 4) with the stirring rate at 410 rpm and 820 rpm, respectively. The same experiment was carried out under different conditions (180.0 V, 2.2 vol% H_2O) to detect its universality, and similar behavior was found.

When the stirring was switched on in the first procedure, the oscillation was immediately better ordered with significantly higher amplitude (~0.9 mA cm^{-2}) and the average current density remained almost unchanged. However, in the second procedure, the oscillation became disordered with stronger amplitude (~1.7 mA cm^{-2}) as soon as the stirring was switched on. In the mean time, the average current density slowly dropped. The minimum current density during each operation was similar to the current density in an anodization under the same voltage at constant stirring rate (820 rpm). Furthermore, the switching on of the stirring resulted in different time responses in the change of the oscillation characteristics (ordering and magnitude) and the average current density, respectively. On one hand, the ordering and magnitude of the oscillation changed almost instantly as the stirring was turned on. On the other hand, the average current density dropped to the minimum much more slowly (several minutes) after the stirring was switched on.

Compared to the other oscillation phenomena in TiO_2 [27, 28] and Al_2O_3 systems [37], this system shows some significant differences. Firstly, the stirring can enhance the current oscillation instead of eliminating it in this fast oscillation. Secondly, the inner surface of the tubes becomes

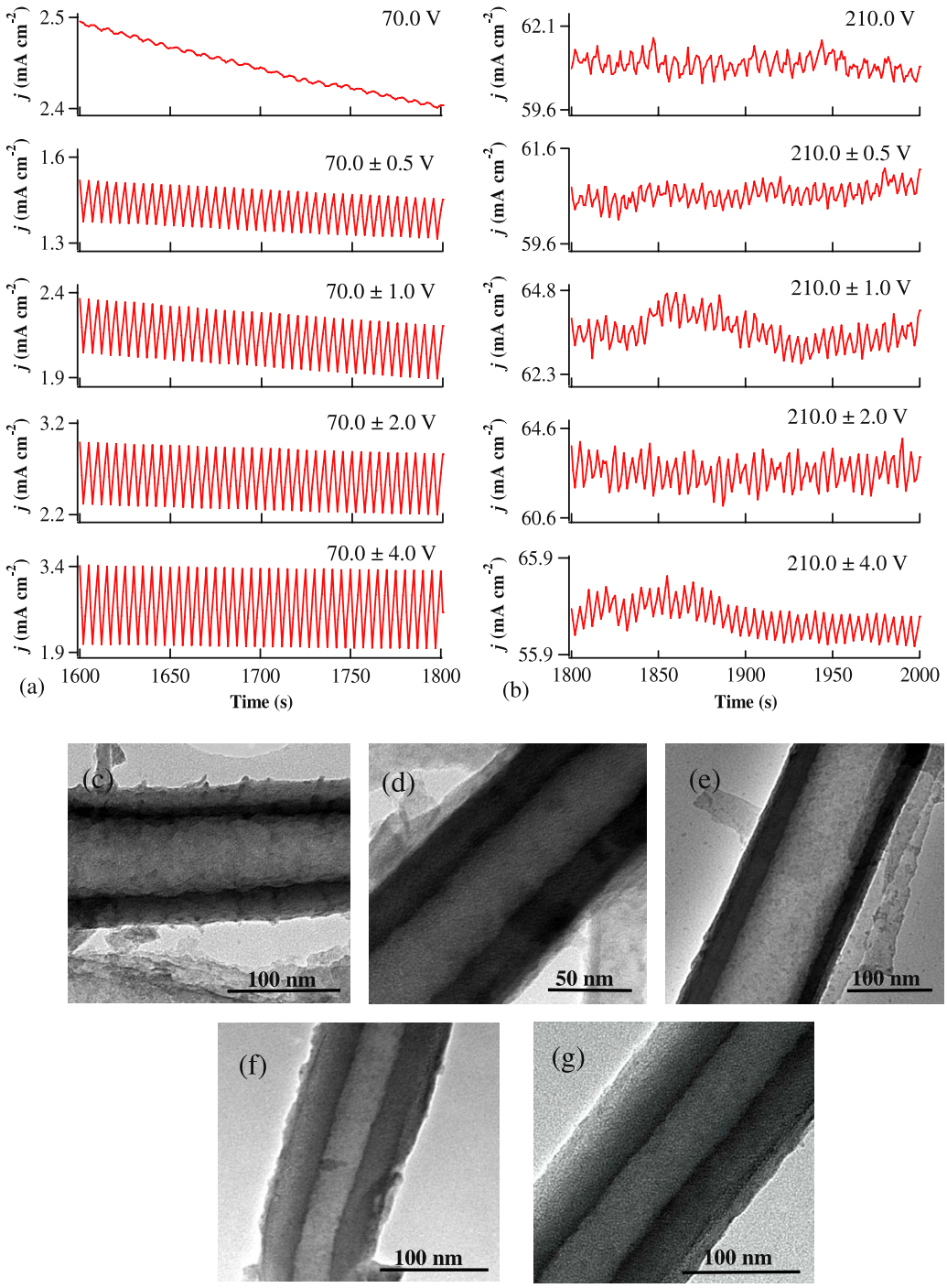

Figure 5. The effect of the modulated voltage on the pore morphology of the TiO_2 tubes, in ethylene glycol (0.09 M NH_4F, 1.0 vol% H_2O), at 5 °C, $\Phi = 450$ rpm. (a), (b) The j–t curve with different modulation amplitudes under low field and high field conditions, respectively. (c)–(g) TEM images taken at the same height at different modulated voltages: (c) 210.0 V; (d) 210.0 ± 0.5 V; (e) 210.0 ± 2.0 V; (f) 70.0 ± 1.0 V; (g) 70.0 ± 4.0 V.

very smooth instead of being rougher with high enough stirring rate, though the current oscillation is chaotic and strong. Furthermore, when the stirring is switched to very high rotation rate (820 rpm), the current slowly drops instead of rising. Finally, when the stirring is switched on, the time responses of the consequent changes of the oscillatory behavior and the average current density are significantly different. In general, a consideration of the transport processes of the ionic species (F^-, O^{2-}, H^+) in this system becomes necessary [29, 30, 41]. Therefore, the involvement of the electric field should also be taken into account and the following experiments with modulated anodic voltages were also conducted.

3.3. The effect of periodical voltage modulation on the current oscillation and the pore morphology

Figure 5 shows the results from the experiments with periodically modulated voltages. The modulation voltage

was triangular shaped and its period was set to 5 s, which was similar to the period in the current oscillation under potentiostatic conditions. The modulation amplitude was much smaller (0–4.0 V) than the average voltage (>70.0 V). As shown in figures 5(a) and (b), the current density curve shows similar oscillation behavior to the voltage. Surprisingly, when the periodical potential was applied, the inner surface of the TiO_2 tubes became smoother than that in the potentiostatic situation, as shown in figures 5(c)–(g). This effect became more significant under higher anodic potential. With higher modulation amplitude of the voltage, the inner surface of the tubes became smoother and the wall thickness became thinner.

Compared to the current oscillation and the pore morphology change mentioned in sections 3.1 and 3.2, no significant pore morphological heterogeneities were induced under the artificially modulated voltage with similar short period (5.0 s). On the contrary, the roughness of the inner surface of the TiO_2 tubes could be totally eliminated with application of the voltage modulation. Considering this result with the result from the stirring experiment, it indicates that the current oscillation and pore morphological change described in section 3.1 are apparently spontaneous. This has further shown that an electric method like modulation of voltages could significantly suppress the roughness in the inner surface of the tube induced by the spontaneous oscillation. It is also interesting to compare this result with the other results using modified voltages [31–33], which normally resulted in significant morphological heterogeneities. Finally, a general mechanistic description of the whole system could then be established based on all these results.

3.4. The mechanism of the current oscillation and the pore morphology evolution in the formation of TiO_2 nanotubes

From the previous sections, several important phenomena have been presented. First, fast current oscillation can spontaneously exist during the anodic growth of TiO_2 tubes, together with various morphology changes inside the tubes. Beside this, there is no simple correlation between the current oscillation and the pore morphological change. Secondly, the current oscillation and the pore morphology can be significantly influenced by the mechanical stirring and the anodic voltage. The switching on of the stirring can induce an instant change in the ordering and magnitude of the current oscillation but a slow decrease of the average current when the stirring rate is very high.

Existing works from the other groups have found that other factors such as the water content, the temperature and the pH value have played an important role in the tube formation in anodization of TiO_2 and other materials [20–33, 37]. However, the temperature, which plays an important role in the oscillation in the Al_2O_3 system [37], is seemingly not a main factor in the oscillatory behavior in this system. This is because the temperature change on the anode is only a few degrees centigrade, and takes place much more slowly than the oscillation in this system. Moreover, the changing of water content apparently does not play a main role in this system due to its low level in this system. Finally, previous experiments have pointed out a key enrollment of the convection layer, which is adjacent to the tubes, in the stirring effect during TiO_2 tube growth [28, 30]. Additionally, some investigations on the capillary tubes have indicated that the transport inside the tubes might also be important for the stirring effects [42]. Therefore, a number of processes should be considered together for the mechanistic description, namely the local reactions of the reactants, the diffusion of the ionic species (O^{2-}, F^-, H^+) and the transport of these species by the outer forces.

Generally, the TiO_2 formation consists of the following well known processes:

$$Ti + 2H_2O = TiO_2 + 4H^+ + 4e \quad (1)$$

$$TiO_2 + 4H^+ + 6F^- = [TiF_6]^{2-} + 2H_2O. \quad (2)$$

Equations (1) and (2) represent the oxidation of Ti and the dissolution of TiO_2, respectively, in which the O^{2-} and F^- ions play an important role [41]. Equation (1) actually contains the generation of O^{2-} (which takes place mostly adjacent to the oxide layer) [30] and its consumption process (which takes place between the oxide layer and the Ti substrate). Both processes are much faster than the diffusion process [29, 30]. The field-aided transport is also considered [30] due to the influence of the modulated voltage on the whole system. Furthermore, the involvement of the $[H^+]$ species (therefore the pH value) should be weak in this system with only small water content ($\leqslant$2.2 vol%) due to its relatively much faster diffusion from the reaction site compared to other species as the F^- and O^{2-}.

To simplify the model, we define $(\frac{\partial[TiO_2]}{\partial t})$ as the change of TiO_2 quantity versus time, in which TiO_2 is treated as one particle for simplification. z is an additional parameter defined as the depth of the ions into the oxide regardless of its position along the tube. Hence the terms $(\frac{\partial[TiO_2]}{\partial t})_{z=0}$ and $(\frac{\partial[TiO_2]}{\partial t})_{z=d}$ correspond to the change of the TiO_2 amount at the inner surface and outer surface of the tube, respectively (normally $(\frac{\partial[TiO_2]}{\partial t})_{z=0} \leqslant 0$ and $(\frac{\partial[TiO_2]}{\partial t})_{z=d} \geqslant 0$). In the area where $0 < z < d$, both the oxidation and dissolution processes are inhibited, hence the change of the TiO_2 thickness Δd is normally proportional to $|(\frac{\partial[TiO_2]}{\partial t})_{z=d}| - |(\frac{\partial[TiO_2]}{\partial t})_{z=0}|$. The relative positions of the inner surface ($z = 0$) and outer surface ($z = d$) to the center of the tube bottom are influenced by different factors. The position of the inner surface is mainly influenced by $[F^-]$, while the position of the outer surface is more strongly influenced by interstitial Ti^{4+} and thus is limited by the anodization voltage [29].

At the bottom of the tube, assume that a stable tube growth is already established (step 1 in figure 6(a)). Stable gradient profiles of the O^{2-} and F^- anions will then be formed [30], and a balance between the oxidation at the inner and outer surface of the TiO_2 wall will be built. As a result, the oxide thickness remains constant. However, this balance is easy to break. When there is a positive perturbation dU in the voltage drop over the sample layer (indicated between step 1 and step 2 in figure 6(a)), an initial rapid increase of the F^- concentration will be immediately induced at the inner surface of the tube. This change will then lead to an increase of $|(\frac{\partial[TiO_2]}{\partial t})_{z=0}|$, i.e., the dissolution of the TiO_2 at the inner surface of the tube is

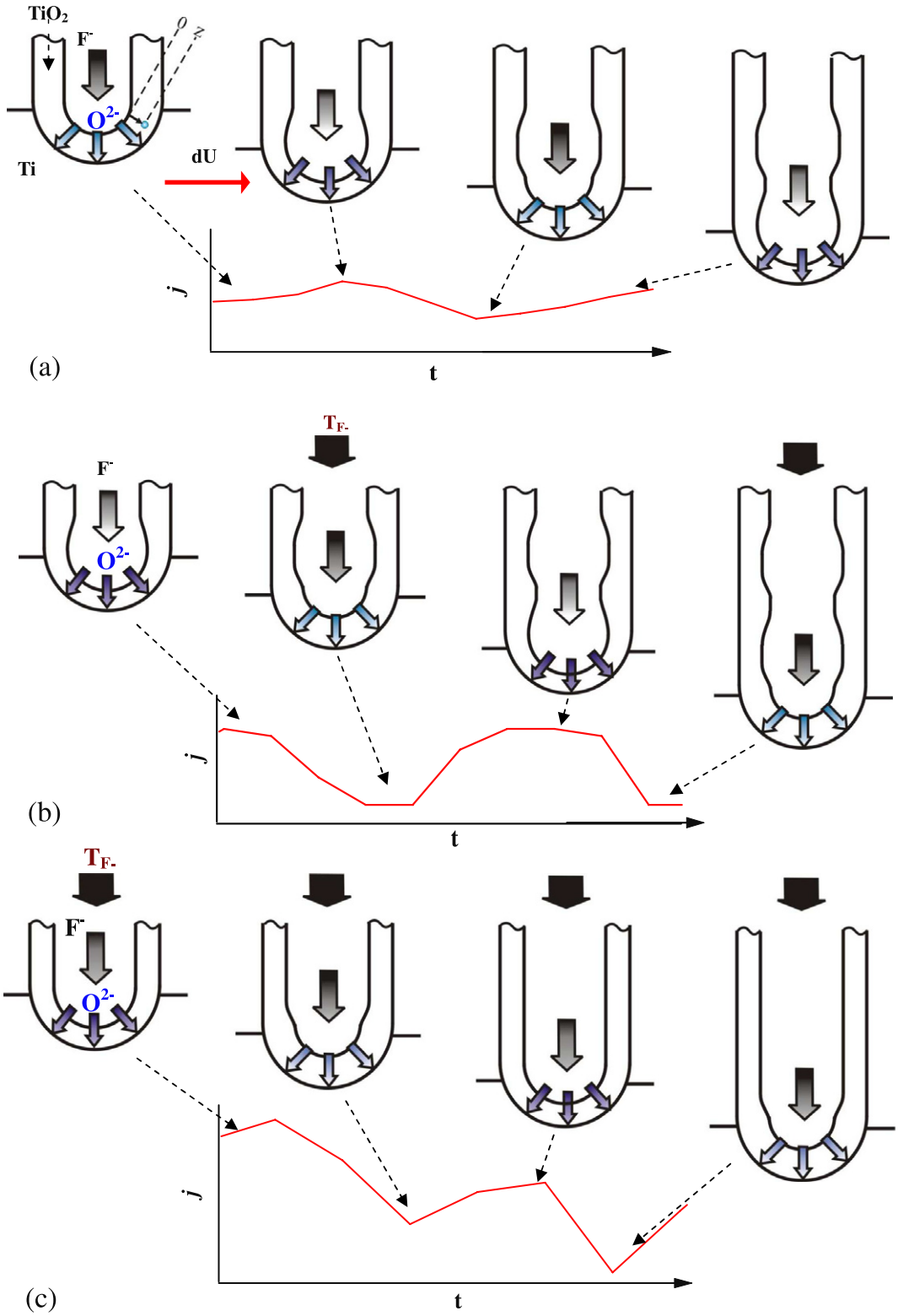

Figure 6. Schematic diagram of the oscillation mechanism: formation of tube spatial periodicity and corresponding current behavior under different conditions: (a) without stirring; (b) at medium stirring rate; (c) at high stirring rate or with periodic modulated voltage. The arrows with gradient represent motion of ion species (F^-, O^{2-}) in the solution and through the oxide. The red arrow in (a) indicates the effect of perturbation. T_F indicates the periodical F^- compensation from the convection layer to the tubes by the stirring or the modulated voltage.

accelerated. However, the change in $|(\frac{\partial[TiO_2]}{\partial t})_{z=d}|$ is much smaller due to much lower $[F^-]$ near the outer surface of the tube bottom. As a result, the tube inner diameter increases at the bottom of the tube and the oxide thickness decreases (from step 1 to step 2 in figure 6(a)). With the decrease of the oxide thickness, on the one hand, $[F^-]$ at the inner surface

($z = 0$) begins to decrease due to the consumption of F^- by the dissolution process indicated by equation (2). On the other hand, the O^{2-} anions will be enriched at the outer surface of TiO_2 due to stronger diffusion and transport through the thinner oxide wall. As a result, the current will begin to increase until it reaches the maximum, as shown in step 2 in figure 6(a).

Secondly, the decrease of the F^- concentration reduces the value of $|(\frac{\partial[TiO_2]}{\partial t})_{z=0}|$. Therefore, the inner diameter of the tube decreases (from step 2 to step 3 in figure 6(a)) and the oxide thickness increases. Compared to the initial state, the inner tube diameter would be slightly smaller due to lower $[F^-]$ at the inner surface with the tube growth. The increase of the oxide thickness induces a decrease of $[O^{2-}]$ at the outer surface, which results in a decreasing current. Furthermore, the voltage drop over the tube layer will increase due to the same reason, so $[F^-]$ at the inner surface is also increased by the field-aided transport. This process continues until both the pore diameter and the current reach the minima, as indicated by step 3 in figure 6(a).

Afterward, due to the enrichment of F^- anions at the inner surface in the bottom of the tubes, $|(\frac{\partial[TiO_2]}{\partial t})_{z=0}|$ is increased. Therefore, the inner diameter of the tube increases and the oxide thickness decreases again. In the meantime, the number of the O^{2-} anions moving through the oxide increases again with the decreasing oxide thickness, so the current rises again (from step 3 to step 4 in figure 6(a)). Finally, the oxide thickness reaches the minimum and the current reaches the maximum, as shown in step 4 in figure 6(a). Due to the F^- consumption during this process, another cycle from step 2 to step 4 will be started afterwards.

If the initial perturbation is negative, the above process will take place vice versa. This means that, after a rapid initial drop of the F^- concentration, the pore diameter first decreases, and then increases with enriched F^-. Finally, it decreases again due to the consumption of F^- anions. In the meantime, the current will be inverse to that with the positive initial perturbation, which is shown in figure 6(a). Nevertheless, the above discussions have only described the situation in a single tube. Both situations should be considered for a total result during a long time growth over the whole substrate. On one hand, these cycles can survive for a long period due to the reduced mobility of the ionic species by the highly viscous electrolyte and the thin TiO_2 tubes. On the other hand, the above processes can take place on the whole substrate by local fluctuations or perturbations from the neighboring tubes, which can be negative or positive. Hence, as a general result, a continuous but weak and chaotic current oscillation is formed together with morphological change in the pore area of the tubes.

When the mechanical stirring is applied, more F^- anions will be periodically transported into the convection layer which is adjacent to the tubes [28, 30]. Then they will soon be transported into the top of the tubes, as indicated by T_{F^-} in figure 6(b). Afterwards, the F^- anions will move to the bottom of the tubes by the diffusion and field-aided transport. These ions can compensate the consumption of the F^- anions from the dissolution process. The F^- anions in the bottom of the tubes will be consumed again soon after each time of such compensation due to the relatively much faster dissolution process inside the tubes compared to the diffusion. Therefore a stable and continuous concentration profile of F^- anions will not result. On the contrary, a periodical compensation of the F^- anions will be established from the top of the tubes (marked by T_{F^-} on top of the figures in figure 6(b)) to the bottom. As a result, the $[F^-]$ at the tube bottom would also change periodically, but the period will be longer than the period of the stirring due to the slow diffusion process inside the tubes. The change of $[F^-]$ in this situation is stronger than that without stirring, which induces stronger influence on the change of the wall thickness. Consequently, the amplitude of the current oscillation becomes higher, while the ordering of the oscillation and the pore morphological change become better. The ordering of the current oscillation and the morphological change will both become the highest when the period of the top-down compensation is so high as to be comparable to the period of the spontaneous cycles discussed in previous paragraphs when no stirring is applied.

When the stirring rate continues to increase (figure 6(c)), on one hand, the motion of O^{2-} will be accelerated. On the other hand, a time mismatch is established between the period of the top-down compensation and the period of the spontaneous cycles when no stirring is applied. Therefore the change of O^{2-} concentration will become stronger but more chaotic. As a consequence, the current oscillation becomes chaotic with higher amplitude. Furthermore, with the increasing stirring rate, the F^- anions at the inner surface of TiO_2 are enriched not only near the tube bottom but also in the area above it. As a result, the previously generated spatial heterogeneities such as the narrowing and the abruption will be dissolved. When a periodically modulated anodic potential is applied, the F^- concentration is significantly increased by stronger field-aided transport, which will also lead to strong dissolution on the inner wall above the tube bottom. Consequently, the roughness in the inner surface will be diminished. This smoothing effect of the inner surface will become stronger if the modulation amplitude is further increased, as shown in figure 5.

The different time responses of the oscillation state and the average current to a sudden 'switching-on' of the stirring, as mentioned in section 3.2, are apparently attributed to different origins. On one hand, the switching-on of the stirring can immediately induce the redistribution of anions in the convection layer above the tube array [28]. This process induces a rapid change in the local electric field, and then changes the state of the current oscillation in a short time. On the other hand, at very high stirring rate, the temperature at the reaction site in the tube arrays is slowly decreased by the high speed stirring, which will slowly decelerate the oxidation process. Therefore, when the stirring is switched on to a very high value, the average current will slowly decrease.

3.5. Applications of the controllable oscillation in nanostructure fabrication

In this work, we have investigated the characteristics and mechanism of the oscillatory behavior in TiO_2 nanotube

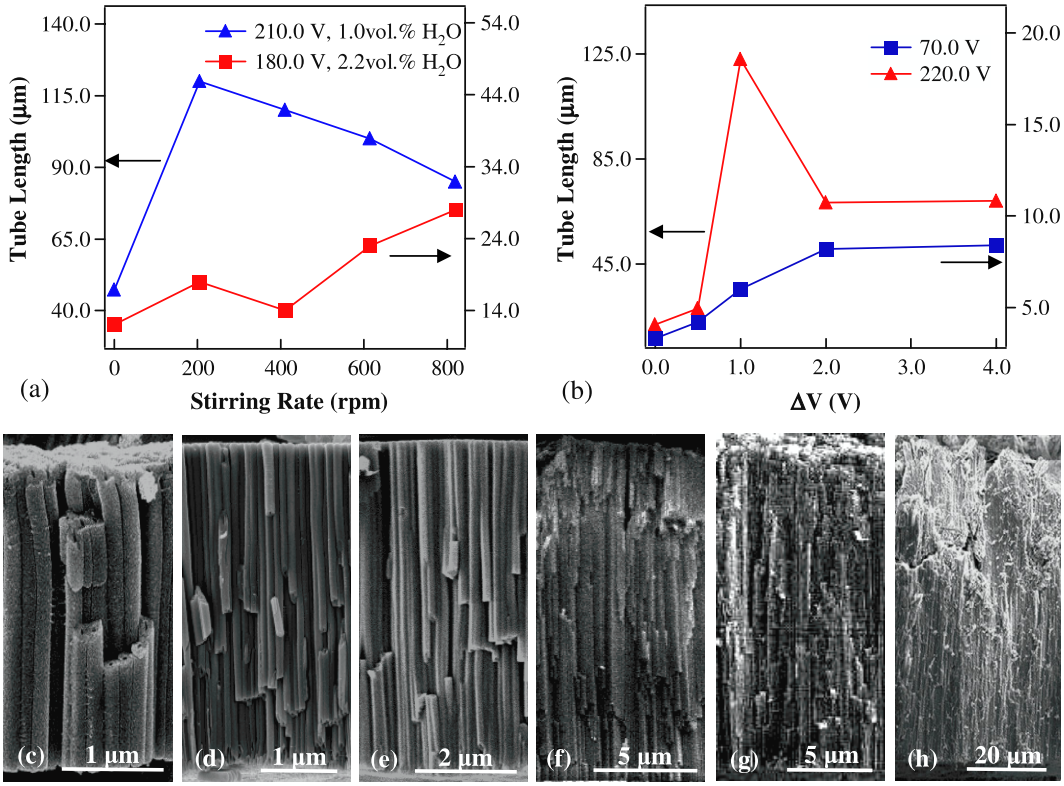

Figure 7. TiO_2 tube growth versus stirring rate and modulation amplitude of the anodization potential, with the anodization time $t_a = 3600$ s, at 5 °C. (a) Tube growth with different stirring rates, in ethylene glycol under different conditions (1.0 vol% H_2O, 180.0 V and 2.2 vol% H_2O, 210.0 V); (b) tube growth at different modulation amplitudes; (c)–(h) SEM images of the TiO_2 tubes anodized at different modulation amplitudes under high and low field conditions, in ethylene glycol (1.0 vol% H_2O, 0.09 M NH_4F): (c) 70.0 V, (d) 70.0 ± 1.0 V, (e) 70.0 ± 4.0 V, (f) 220.0 V, (g) 220.0 ± 0.5 V, (h) 220.0 ± 1.0 V.

formation. It has been found that the pore morphology of the TiO_2 tubes can be significantly affected in a certain way by simply changing the parameters of the mechanical stirring or the voltage modulation. Therefore it is likely to be useful to control the oscillatory behavior in various applications.

Firstly, straight tubes with smooth inner surface can be fabricated with the inhibition of the roughness generation in the pore area of the tubes. These tubes may have better absorption ability for dye molecules or nanoparticles, and may improve their performance in the opto-electronic devices. The inhibition of the pore roughness could be realized by applying high stirring rate or modulating the anodization voltage with relatively higher amplitude, according to our previous results in figures 3–5.

Secondly, from the discussion in section 3.4, it is likely that tube growth could be also accelerated due to strengthened ion compensation at the bottom with the smoother tubes. This is supported by the results represented in figures 7(a) and (b). On one hand, when the stirring was applied, the TiO_2 tubes were grown faster with higher stirring rate in a certain range in a fixed anodization time (in this work the period is 1 h), as shown in figure 7(a), and with different water content in the electrolyte the monotonicity of the growth rate versus the stirring rate was different under various conditions. With higher water concentration (2.2 vol%), the growth rate increased monotonically with the increasing stirring rate. However, with lower water concentration (1.0 vol%), it first increased and then slowly decreased with the increasing stirring rate. On the other hand, when a periodically modulated potential was applied, the tube growth was generally accelerated, as shown in figure 7(b). Furthermore, the tube length in a constant growth time (1 h) increased monotonically with the increasing modulation amplitude ΔV under low field conditions (70.0 V), but under high field conditions (220.0 V) it first increased and then decreased again with increasing ΔV. Additionally, the quality of the tubes was also improved with the modulated voltages, as shown in figures 7(c)–(h).

As a result, a combination of the mechanical stirring and modulated voltage is likely to further improve the tube growth rate with smooth surface in the pore, which might be useful in fabrication of high efficiency solar cells or other devices [2–9]. Furthermore, according to previous results, TiO_2 tubes with some certain periodicity in the pore area may also be fabricated when the stirring is limited in a moderate rate (~410 rpm) at high voltages (normally between 160.0 and 220.0 V). These tubes may be applicable as templates [37] or functional materials for other physical and biochemical devices [22] due to their own semiconducting and catalytic properties.

Table 1. A general summary of the current oscillation and the pore morphological evolution under different stirring and voltage modulation conditions.

	Mechanical stirring Φ				Voltage modulation ΔU	
	No stirring	Low stirring (0–300 rpm)	Medium stirring (300–512 rpm)	Strong stirring ($\geqslant$512 rpm)	$\Delta U = 0$	$\Delta U > 0$
Oscillation amplitude	Very small	Small	Medium	High	Medium[a]	Proportional to ΔU
Oscillation ordering	Chaotic	Less chaotic	Ordered	Chaotic	Ordered[a]	Ordered, similar to the modulation
Surface in the pore	Rough	Rough	With certain periodicity	Smooth	Not smooth[a]	Smooth
Change of the growth rate	0[b]	>0	>0	>0	0[b]	>0

[a] States as references, taken under constant stirring rate ~450 rpm. [b] Default states as a reference for comparison.

4. Conclusions

In this paper, we have introduced a new kind of current oscillation with pore morphological change in the growth of anodic TiO_2 nanotubes which is controllable by stirring and anodic voltage. The characteristic timescale of the oscillation is about 10^0 s and its amplitude is less than 8.0% of the minimum current. The morphological change (the narrowing, abruption and shallow pits) in the pore area of the tubes has a characteristic length scale of $\sim 10^1$–10^2 nm. These properties indicate a latent relationship with the previously observed morphological heterogeneities during the normal anodic growth of TiO_2. It has been found in further investigation that this oscillatory behavior can be controlled by a few key macroscopic experimental factors, namely the stirring rate and the voltage modulation amplitude. For instance, ordered current oscillation with a certain periodicity in the pore could be obtained by limiting the stirring around the medium value (~410 rpm). Moreover, the inner surface of the tubes could be smoothed by high speed stirring or periodically modulated anodic voltage, though the current oscillation became stronger and more chaotic. Finally, stirring with higher rate and voltage with small modulation amplitude can lead to a significantly higher growth rate, which can be about two to three times faster than the tube growth without control. These phenomena have been exhibited in table 1 to give a general summary.

Based on the experimental results, the mechanism has been discussed with the consideration of the local reactions and transport processes of the main reaction species. Under this interpretation, the current oscillation and the morphology change in the pore are attributed to the redistribution of the ionic species by the fluctuation in the tube layer when there is no stirring. They can be significantly influenced by the convection above the tube layer and the slow transport process (diffusion and field-aided transport) in the tubes with the existence of mechanical stirring or voltage modulation. The smoothing effect of the tube inner surface and the acceleration of the growth are due to the redistribution of the F^- anions in the bottom of the tubes, which is influenced by the stirring and modulated voltage via the slow transport process. Hence, besides the direct applications of the results, this work has also probed a way to investigate the nanostructure formation, which can hopefully help the development of nanostructure fabrication methods in general.

Acknowledgments

This work was supported by the National Major Basic Research Project 2010CB933702, Natural Science Foundation of China, under contracts 10734020 and 11074169.

References

[1] Zwilling V, Darque-Ceretti E, Boutry-Forveille A, David D, Perrin M Y and Aucouturier M 1999 *Surf. Interface Anal.* **27** 629
[2] Fujishima A and Honda K 1972 *Nature* **238** 37
[3] O'Regan B and Grätzel M 1991 *Nature* **353** 737
[4] Mor G K, Shankar K, Paulose M, Varghese O K and Grimes C A 2006 *Nano Lett.* **6** 215
[5] Kitao M, Oshima Y and Urabe K 1997 *Japan. J. Appl. Phys.* 1 **36** 4423
[6] Albu S P, Ghicov A, Macak J M and Schmuki P 2007 *Nano Lett.* **7** 1286
[7] Tsuchiya H, Macak J M, Müller L, Kunze J, Müller F, Greil P, Virtanen S and Schmuki P 2006 *J. Biomed. Mater. Res.* A **77A** 534
[8] Balaur E, Macak J M, Tsuchiya H and Schmuki P 2005 *J. Mater. Chem.* **15** 4488
[9] Grimes C A and Mor G K 2009 *TiO_2 Nanotube Arrays: Synthesis, Properties and Applications* (New York: Springer) p 318
[10] Macak J M and Schmuki P 2006 *Electrochim. Acta* **52** 1258
[11] Macak J M, Tsuchiya H, Taveira L, Aldabergerova A and Schmuki P 2005 *Angew. Chem. Int. Edn* **44** 7463
[12] Wang J and Lin Z Q 2008 *Chem. Mater.* **20** 1257
[13] Prakasam H E, Shankar K, Paulose M, Varghese O K and Grimes C A 2007 *J. Phys. Chem.* C **111** 7235
[14] Nagaveni K, Hegde M S, Ravishankar N, Subbanna G N and Madras G 2004 *Langmuir* **20** 2900
[15] Masuda H and Fukuda K 1995 *Science* **268** 1466
[16] Huang Z, Zhang X, Reiche M, Liu L, Lee W, Shimizu T, Senz S and Gösele U 2008 *Nano Lett.* **8** 3046
[17] Qin L, Park S, Huang L and Mirkin C A 2005 *Science* **309** 113
[18] Yin H, Liu H and Shen W Z 2010 *Nanotechnology* **21** 035601
[19] Yasuda K and Schmuki P 2007 *Electrochim. Acta* **52** 4053
[20] Valota A, LeClere D J, Skeldon P, Curioni M, Hashimoto T, Berger S, Kunze J, Schmuki P and Thompson G E 2009 *Electrochim. Acta* **54** 4321
[21] Berger S, Kunze J, Schmuki P, Valota A T, Leclere D J, Skeldon P and Thompson G E 2010 *J. Electrochem. Soc.* **157** C18
[22] Song Y-Y and Schmuki P 2010 *Electrochem. Commun.* **12** 579
[23] Albu S P, Ghicov A, Macak J M and Schmuki P 2007 *Phys. Status Solidi RRL* **1** R65
[24] Paulose M, Shankar K, Yoriya S, Prakasam H E, Varghese O K, Mor G K, Latempa T A, Fitzgerald A and Grimes C A 2006 *J. Phys. Chem.* B **110** 16179

[25] Macak J M, Zlamal M, Krysa J and Schmuki P 2007 *Small* **3** 300
[26] Valota A, LeClere D J, Skeldon P, Curioni M, Hashimoto T, Berger S, Kunze J, Schmuki P and Thompson G E 2009 *Electrochim. Acta* **54** 4321
[27] Macak J M, Albu S, Kim D H, Paramasivam I, Aldabergerova S and Schmuki P 2007 *Electrochem. Solid-State Lett.* **10** K28
[28] Kim D, Schmidt-Stein F, Hahn R and Schmuki P 2008 *Electrochem. Commun.* **10** 1082
[29] Macak J M, Hildebrand H, Marten-Jahns U and Schmuki P 2008 *J. Electroanal. Chem.* **621** 254
[30] Macak J M, Tsuchiya H, Ghicov A, Yasuda K, Hahn R, Bauer S and Schmuki P 2007 *Curr. Opin. Solid State Mater. Sci.* **11** 3
[31] Chanmanee W, Watcharenwong A, Chenthamarakshan C R, Kajitvichyanukul P, De Tacconi N R and Rajeshwar K 2008 *J. Am. Chem. Soc.* **130** 965
[32] Albu S P, Kim D and Schmuki P 2008 *Angew. Chem. Int. Edn* **47** 1916
[33] Kim D, Ghicov A, Albu S P and Schmuki P 2008 *J. Am. Chem. Soc.* **130** 16454
[34] Taveira L V, Macak J M, Sirotna K, Dick L F P and Schmuki P 2006 *J. Electrochem. Soc.* **153** B137
[35] Yasuda K, Macak J M, Berger S, Ghicov A and Schmuki P 2007 *J. Electrochem. Soc.* **154** C472
[36] Parkhutik V, Curiel-Esparza J, Millan M-C and Albella J 2005 *Phys. Status Solidi* a **202** 1576
[37] Lee W, Kim J-C and Gösele U 2009 *Adv. Funct. Mater.* **20** 21
[38] Haken H 1978 *Synergetics: Introduction and Advanced Topics* (Berlin: Springer) pp 275–304
[39] Imbihl R and Ertl G 1995 *Chem. Rev.* **95** 697
[40] Zhang F, Chen S G, Yin Y S, Lin C and Xue C R 2010 *J. Alloys Compounds* **490** 247
[41] Ghicov A and Schmuki P 2009 *Chem. Commun.* **20** 2791
[42] Backofen U, Hoffman W and Matysik F-M 1998 *Anal. Chim. Acta* **362** 213